Tuning of power system stabilizer for small signal stability improvement of interconnected power system

Prasenjit Dey, Aniruddha Bhattacharya and Priyanath Das
Department of Electrical Engineering, National Institute of Technology Agartala, West Tripura, India

Received 7 September 2017
Revised 19 December 2017
Accepted 28 December 2017

Abstract
This paper reports a new technique for achieving optimized design for power system stabilizers. In any large scale interconnected systems, disturbances of small magnitudes are very common and low frequency oscillations pose a major problem. Hence small signal stability analysis is very important for analyzing system stability and performance. Power System Stabilizers (PSS) are used in these large interconnected systems for damping out low-frequency oscillations by providing auxiliary control signals to the generator excitation input. In this paper, collective decision optimization (CDO) algorithm, a meta-heuristic approach based on the decision making approach of human beings, has been applied for the optimal design of PSS. PSS parameters are tuned for the objective function, involving eigenvalues and damping ratios of the lightly damped electromechanical modes over a wide range of operating conditions. Also, optimal locations for PSS placement have been derived. Comparative study of the results obtained using CDO with those of grey wolf optimizer (GWO), differential Evolution (DE), Whale Optimization Algorithm (WOA) and crow search algorithm (CSA) methods, established the robustness of the algorithm in designing PSS under different operating conditions.

Keywords Collective decision optimization, Damping ratio, Power system stabilizer, Small signal stability
Paper type Original Article

1. Introduction
Power system is a highly complex and non-linear system and it has always suffered from low frequency oscillations ranging from 0.2 to 2 Hz [1]. These troublesome dynamic oscillations arise due to various disturbances like load variations, line outages and also some other factors like characteristics of various control devices and electrical connections between the components. Due to these low frequency oscillations power-transfer capability of power systems get reduced. Moreover they are associated to the rotor angle of the synchronous

The authors would like to acknowledge the Department of Electrical Engineering, NIT Agartala for providing laboratory facilities.

Publishers note: The publisher wishes to inform readers that the article “Tuning of power system stabilizer for small signal stability improvement of interconnected power system” was originally published by the previous publisher of Applied Computing and Informatics and the pagination of this article has been subsequently changed. There has been no change to the content of the article. This change was necessary for the journal to transition from the previous publisher to the new one. The publisher sincerely apologises for any inconvenience caused. To access and cite this article, please use Dey, P., Bhattacharya, A., Das, P. (2020), “Tuning of power system stabilizer for small signal stability improvement of interconnected power system”, Applied Computing and Informatics. Vol. 16 No. 1/2, pp. 3-28. The original publication date for this paper was 29/12/2017.

Applied Computing and Informatics
Vol. 16 No. 1/2, 2020
pp. 3-28
Emerald Publishing Limited
e-ISSN: 2210-8327
p-ISSN: 2634-1964
DOI 10.1016/j.aci.2017.12.004

machines which continues to grow causing loss of synchronism if adequate damping is not provided to the system. So power system stabilizers are most commonly used to damp out the system oscillations and also to enhance the damping of electromechanical modes. These oscillations can be divided into two main important categories: firstly the local mode of oscillations, ranging from 0.8 to 2 Hz and inter area mode of oscillations ranging from 0.2 to 0.8 Hz. These phenomena can be examined by eigenvalue analysis and can be solved with the help of power system stabilizer. Suitably tuned parameters of PSS introduce a component of electrical torque which is in phase with the generator rotor angle deviations and can damp out low frequency oscillations. Inputs to the stabilizer can be rotor frequency, rotor speed deviation and accelerating power, etc. High gain automatic voltage regulators are used in excitation systems which invites low frequency oscillations in the system. In [2] proportional integral derivative controller have been used which provides modulated signal to AVR for damping out the low frequency oscillations. Literature survey shows that many conventional power system stabilizers (CPSS) [3] have been considered consisting of lead-lag compensators. The design of such CPSS involves the linearized dynamic model which is based on linear control theory and gives poor performance under varying operating conditions. Also it fails to maintain stability of electrical power system when subjected to high loading conditions. Despite satisfactory performance of classical approaches like H-infinity [4], LMI [5], and pole placement [6] techniques, meta-heuristic techniques are more popular due to their simplicity of implementation and less computational efforts over the classical techniques in finding the optimal solution. Moreover, real life problems including design optimization problems make use of several types of variables, objective functions, and constraint functions simultaneously in their formulation. Classical techniques are not suitable for complex non-convex, non-smooth, and non-differentiable objective functions and constraints. To overcome these problems, heuristic algorithms are sought after as they are capable of solving the non-linear problems. Recently various Artificial Intelligent (AI) techniques are being used for mitigating the problem related to low frequency oscillations. Among the several AI techniques, artificial neural network (ANN) [7–11] has been widely used for designing PSS. But ANN based controllers are limited by their longer training period and in the selection of numeral of layers and also, neurons for each of the layers. Fuzzy logic controller (FLC) is also one of the AI techniques that have gained attention for controlling PSS signal [12–14]. The main advantage of FLC is that it can provide control signal to the plant which is based on linguistic rules derived from the operator. FLC's can be designed by making use of linguistic information obtained earlier from the control system and hence, accurate model of the plant is not required. But problem with this controller is that, it requires hard work and fine tuning to achieve adequate signal. Recently, evolutionary based optimization techniques are gaining more attention for designing of power system stabilizer. Conventional PSS has been designed using various techniques like Genetic algorithm (GA) [15–16], Particle swarm optimization (PSO) [17–19], differential evolution (DE) [20–21], firefly algorithm (FA) [22], cuckoo search (CS) [23], evolutionary programming [24], tabu search [25], simulated annealing [26], BAT [27] and rule based bacteria foraging [28].

Here, a new metaheuristic algorithm called collective decision optimization (CDO) [29] for tuning PSS parameters in a multi machine power system has been presented. State space representation of the system is done for performing small signal stability analysis. WSCC 3 machine 9 bus and IEEE 14 bus systems are considered as test systems. There are various methods available for small signal stability analysis, such as Eigen value analysis, synchronizing and damping torque analysis, frequency response and residue based analysis. Behavior of the system has been studied with the help of eigenvalue analysis because of its simplicity and efficiency over other techniques. The main advantage of eigenvalue technique is that it can easily identify various electromechanical modes which are otherwise very difficult to obtain with other mentioned techniques. Also, the oscillations can be characterized very easily and accurately. Results so obtained by this algorithm is compared with other optimization techniques like GWO, DE, WOA and CSA which shows that this proposed technique enhances overall stability and mitigates the problem related to low frequency oscillations.

2. Dynamics of power system

The d–q axis transformation of synchronous machines has been considered for representing dynamics of power system [30]. For large interconnected systems, the network is usually considered as a constant impedance matrix including the loads. Generator fourth order model consisting of four states have been considered for modeling synchronous machine and fast acting exciter or static exciter as excitation system. The state equations are modeled as shown in [31].

2.1 Generator equations

$$\dot{\delta} = \omega_i - \omega_s \tag{1}$$

$$\dot{\omega} = \frac{T_{Mi}}{M_i} - \frac{\left[E'_{qi} - X'_{di} I_{di}\right] I_{qi}}{M_i} - \frac{\left[E'_{di} - X'_{qi} I_{qi}\right] I_{di}}{M_i} - \frac{D_i(\omega_i - \omega_s)}{M_i} \tag{2}$$

$$\dot{E}_{qi'} = -\frac{E'_{qi}}{T'_{doi}} - \frac{(X_{di} - X'_{di}) I_{di}}{T'_{doi}} + \frac{E_{fdi}}{T'_{doi}} \tag{3}$$

$$\dot{E}'_{di} = -\frac{E'_{di}}{T'_{qoi}} - \frac{\left(X_{qi} - X'_{qi}\right) I_{qi}}{T'_{qoi}} \tag{4}$$

2.2 Exciter equation

$$\dot{E}_{fdi} = -\frac{E_{fdi}}{T_{Ai}} + \frac{K_{Ai}}{T_{Ai}} (V_{refi} - V_i + V_{si}) \tag{5}$$

These above mentioned set of nonlinear equations can be represented as follows:

$$\dot{X} = f(X, U) \tag{6}$$

where X denotes state vectors given by $X = [\delta, \omega, E'_q, E'_d, E_{fd}]^T$ and U denotes the input vector which is the PSS output signal in this case. δ, ω, E'_q, E'_d, E_{fd} denote respectively the rotor angle, speed, internal voltage along quadrature axis and direct axis and field voltage respectively. These equations can be represented in state space form and are given below:

$$\dot{X} = AX + BU \tag{7}$$

Here generator 4th order model and static exciter are considered. So the dimension of A matrix is $5m \times 5m$ and B matrix is $5 \times n$, where, m and n denotes the number of machines and number of PSS installed in the system respectively.

Investigation is done by considering various operating conditions like loading conditions, line outages etc. Different loading conditions are presented in (Tables 1 and 2) for both WSCC 3 machine 9 bus and IEEE 14 bus system respectively. Detailed system data has been taken from [32,33]. Figures 1 and 2 represents single line diagram for the above mentioned test systems. As far as small signal stability is concerned, it always deals with finding electro mechanical modes as well as state variables which participate effectively in the system. So, various modes of oscillations can be identified by the use of participation factors [34].

Table 1. Different loading conditions (p.u), for WSCC 3 machine 9 bus system.

	Lightly loaded		Normally loaded		Heavily loaded	
	P	Q	P	Q	P	Q
Generator						
G1	0.9649	0.2330	1.7164	0.6205	3.5730	1.8143
G2	1.0000	−0.1933	1.6300	0.0665	2.2000	0.7127
G3	0.4500	−0.2668	0.8500	−0.1086	1.3500	0.4313
Load						
L5	0.7000	0.3500	1.2500	0.5000	2.0000	0.9000
L6	0.5000	0.3000	0.9000	0.3000	1.8000	0.6000
L8	0.6000	0.2000	1.0000	0.3500	1.6000	0.6500
Local load at G1	0.6000	0.2000	1.0000	0.3500	1.6000	0.6500

Table 2. Different loading conditions (p.u), for IEEE 14 bus system.

	Lightly loaded		Normally loaded		Heavily loaded	
	P	Q	P	Q	P	Q
Load						
L4	0.4000	0.1233	0.8000	0.1900	1.4000	1.3248
L5	0.0450	−0.2095	0.0900	0.0160	0.1000	1.1009
L9	0.1200	−0.1452	0.3500	0.1660	0.6000	0.5648

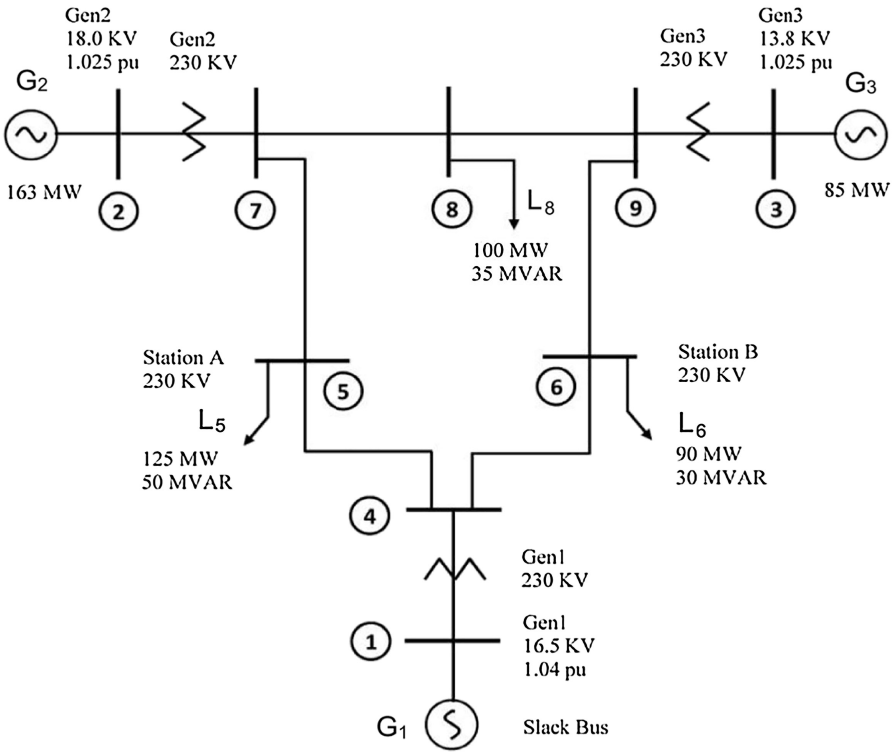

Figure 1. WSCC 3 machine 9 bus system [31].

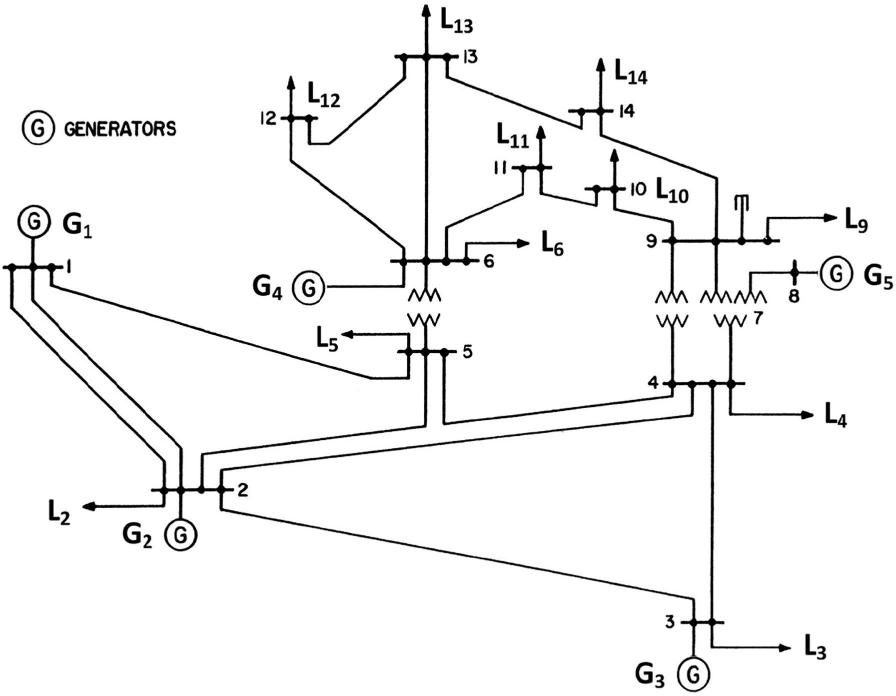

Figure 2. Single line diagram for IEEE 14 bus system.

3. Power system stabilizer

The function of PSS is to provide an additional torque to the exciter to damp out low frequency oscillations. The most commonly used PSS is speed based (CPSS). Throughout the study, CPSS is considered for designing purpose. Figure 3 shows the functional block diagram of CPSS.

The above diagram represents a two staged PSS, consisting of a gain block, a washout circuit and dynamic compensator. In the gain block, K_{PSS} is nothing but gain of the PSS usually ranging from 0.01 to 50 [35]. Gain of PSS is an important factor as it is responsible for providing adequate damping torque. Damping provided by PSS is proportional to the gain until it reaches critical values, after which damping start decreasing. Washout circuit acts as a high-pass filter. It passes all the required frequencies and eliminates steady-state signals in the output of PSS which otherwise modifies generator terminal voltage. T_w is the time constant of washout filter. Previous works show that, for noticeable improvement of system damping, one has to consider T_w as 10 seconds (s) [36]. Phase lead-lag compensation block can compensate for the lag between PSS output and electrical torque and also eliminate the delay between excitation and electrical torque. The transfer function of PSS can be expressed as:

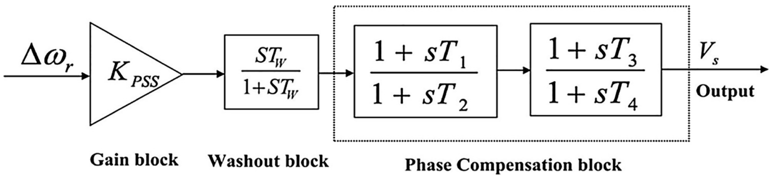

Figure 3. Block diagram of two staged PSS.

$$G_{PSS}(s) = \frac{V_{si}(s)}{\omega_i(s)} = K_{PSSi} \cdot \left[\frac{sT_{Wi}}{1+sT_{Wi}}\right] \cdot \left[\frac{1+sT_{1i}}{1+sT_{2i}}\right] \cdot \left[\frac{1+sT_{3i}}{1+sT_{4i}}\right] \tag{8}$$

where speeds deviation is taken as the input signal to the PSS.

4. Problem formulation

When power system is subjected to any disturbance, the decaying rate of oscillation is taken care of by damping factors of the system and the amplitude is determined by the damping ratio. Two sub objective functions have been considered here for tuning PSS parameters and the assessment is done using eigenvalue analysis. First sub objective function considers minimizing real part of eigenvalue and second part, considers maximizing the damping ratio, as shown in [35]. Eigenvalue having larger negative real part with higher value of damping ratio ensures a stable system. The damping co-efficient is derived from real and oscillatory parts of eigenvalues. The objective function contains real part of the eigenvalues as well as the damping co-efficient in order to tune PSS parameters. Therefore main objective is to improve the real part of eigenvalues and damping ratio. Mathematically it can be represented as:

$$\text{Minimize } I = I_1 + I_2 \tag{9}$$

where

$$I_1 = \sum_{i=1}^{n} (\sigma_0 - \sigma_i)^2; \quad I_2 = \sum_{i=1}^{n} (\zeta_0 - \zeta_i)^2; \tag{10}$$

Here, n is the number eigenvalues that is associated with the electromechanical modes. I_1 represents the objective function related to real part of eigenvalues that leads them towards left half of S plane and I_2 refers to the improvement of damping ratios. σ represents the real part and ζ, the damping ratio of the eigenvalues. Values of σ_0 and ζ_0 are taken as -2.5 and 0.1 respectively [17]. T_1 and T_3 are phase-lead time constants and vary in the range of 0.1–1.5s [36]. T_2 and T_4 are phase-lag time constants and vary between 0.01 and 0.15 s [36]. Five parameters namely, K_{PSS}, T_1, T_2, T_3 and T_4 are optimized using different optimization techniques and T_w is kept constant at 10 s. The effect of the objective function is shown in Figure 4. All the optimization techniques considered in this paper has been applied to the objective function described using (9) subject to following inequality constraints.

$$\left.\begin{array}{c} K_{PSS}^{\min} \le K_{PSS} \le K_{PSS}^{\max} \\ T_1^{\min} \le T_1 \le T_1^{\max} \\ T_2^{\min} \le T_2 \le T_2^{\max} \\ T_3^{\min} \le T_3 \le T_3^{\max} \\ T_4^{\min} \le T_4 \le T_4^{\max} \end{array}\right\} \tag{11}$$

This paper mainly focuses on CDO, GWO, DE, WOA and CSA algorithms for tuning PSS parameters to improve system stability under different operating conditions.

5. An overview of recently developed optimization

In the last few years some popular optimization algorithms have been developed. All these algorithms are equally effective to solve complex optimization problem. These are CSA, WOA, DE, GWO and CDO, etc. Brief descriptions of these algorithms are given below.

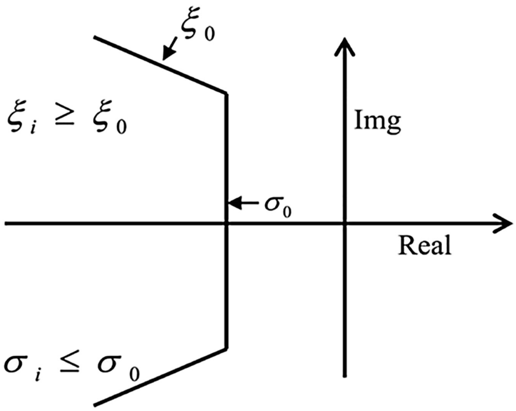

Figure 4.
Region of eigenvalue locations for objective function *I* [37].

5.1 Crow search algorithm

Crow search algorithm, as developed by A. Askarzadeh [38], is a metaheuristic algorithm designed to handle constrained optimization problems. It exploits the intelligent behavior of crows in searching and obtaining food. Crows are assumed to hide any excess food and feed on them as and when required. They are also known to follow other crows to their hideouts and steal their food. It is also assumed that the crows which committed thievery become extra cautious regarding their hideouts so that their food can't be stolen.

In CSA, exploitation and exploration are mainly controlled by the parameter of awareness probability (*AP*) of crows, i.e., if it is being followed by another crow. If it is aware of being followed, then it will assume any random position rather than going to its hideout. For decreased awareness probability value, CSA conducts its search locally, where a present good solution is obtained. Hence, low values of *AP*, increases exploitation capability. Increased *AP* value results in the probability of conducting global search (randomization). As a result, use of large values of AP increases exploration capability of the algorithm.

5.1.1 Pseudo-code for CSA.

Initialize randomly the positions of N crows in search space.
Analyze the position of crows
Initialize memory (m) of the crows in the flock
while *termination criteria not satisfied (iter < maxiter)*
  for *i = 1: N*
    Choose randomly jth crow to follow
    Set awareness probability (AP)
      if $r_j \geq AP^{j,iter}$
        $k^{i,iter+1} = k^{i,iter} + r_i \times fl^{i,iter} \times \left(m^{j,iter} - k^{i,iter}\right)$; *fl = flight length*
      else
        $k^{i,iter+1}$ = *any random position in the search space*
      end
  end
Check feasibility of the new positions attained by crows
Analyze the new positions
Update crows' memories
end

5.2 Whale optimization algorithm

Whale optimization algorithm duplicates the hunting strategies of humpback whales. They employ bubble net mechanism for hunting their preys. Their hunting strategy is close to that of grey wolves and involves the following phases [39]:

5.2.1 Encircling prey. In this phase, it is assumed that the whales have knowledge about the best position of their preys in the search space. After defining the best search agent, the other search agents update their positions towards the best search agent as follows:

$$\vec{D} = |\vec{C}\cdot\vec{X}*(t) - \vec{X}(t)| \tag{12}$$

$$\vec{X}(t+1) = \vec{X}*(t) - \vec{A}\cdot\vec{D} \tag{13}$$

where $\vec{D}$ represents a difference vector, t represents the present time. $\vec{A}$ and $\vec{C}$ are coefficient vectors. $\vec{X}$ and $\vec{X}_p$ represent respectively positions of the whale and the prey. Following equations calculate the coefficient vectors $\vec{A}$ and $\vec{C}$:

$$\vec{A} = 2\cdot\vec{a}\cdot\vec{r}_1 - \vec{a} \tag{14}$$

$$\vec{c} = 2\cdot\vec{r}_2 \tag{15}$$

where $\vec{r}_1$ and $\vec{r}_2$ are random numbers in the interval [0, 1] and components of $\vec{a}$ are linearly decreased from 2 to 0 iteratively.

5.2.2 Bubble – Net attacking method. This is the exploitation phase of the algorithm. Two approaches have been given in [39] for mathematically representing the attacking method of whales which are as follows:

5.2.2.1 Shrinking encircling. This is obtained by decreasing the value of $\vec{a}$ in (14), which in turn results in decrease in the range of $\vec{A}$. New position of whales can be set anywhere between their original position and the present best position by setting $\vec{A}$ randomly within the interval [−1, 1].

5.2.2.2 Spiral updating position. It first calculates the distance between whale and prey and then creates a spiral equation mimicking the helical motion of humpback whales:

$$\vec{X}(t+1) = \vec{D}'\cdot e^{ck}\cdot\cos(2\pi k) + \vec{X}*(t) \tag{16}$$

where $\vec{D}' = |\vec{X}*(t) - \vec{X}(t)|$ represents the distance of ith whale with respect to the prey, c is a constant denoting shape of the spiral and k is any random number in the interval [−1, 1].

Assuming a 50% chance of the whales to adopt either shrinking encircling or spiraling method, their positions are updated as follows:

$$\left.\begin{aligned}\overline{X}(t+1) &= X^{\rightarrow}*(t) - A^{\rightarrow}\cdot D^{\rightarrow} & \text{if } p < 0.5\\ &= D^{\rightarrow\prime}\cdot e^{ck}\cdot\cos(2\pi k) + X^{\rightarrow}*(t) & \text{if } p \leq 0.5\end{aligned}\right\} \tag{17}$$

where p is a random number within the interval [0, 1].

5.2.3 Search for prey. This phase represents the exploration of the whales. This phase also works by varying $\vec{A}$ to search for prey. Whales search randomly in positions relative to one another. In this phase, position of each search agent is updated with respect to a randomly chosen whale instead of the best position, thereby enhancing exploration and allowing for global search. In his phase, $\vec{A} > 1$. The following equations represent mathematical modeling of the phase:

$$\vec{D} = \left|\vec{C}\cdot\vec{X}_{rand} - \vec{X}\right| \tag{18}$$

$$\vec{X}(t+1) = \vec{\vec{X}}_{rand} - \vec{A}\cdot\vec{D} \tag{19}$$

where $\overrightarrow{\overrightarrow{X}}_{rand}$ represents position of any whale chosen randomly from the present population.

5.2.4 Pseudo-code for whale optimization algorithm.

```
Randomly initialize whales (search agents) population X_i (i = 1,
  2, . . . , n) and the maximum number of iteration (maxiter)
Analyze fitness of each search agent
Set X* = best search agent
while (iter < maxiter)
  for i = 1: n
  Update a, A, C, k and p
    if p < 0.5
      if |A| < 1
        update position of present search agent using (12)
      elseif |A| ≥ 1
        Select a random search agent X_rand
        Update position of present search agent using (19)
      end
    else if p ≥ .5
        Update position of present search agent using (16)
    end
  end
  Check if all the search agents lie within the search space
  Analyse fitness of each search agent
  Update X* for any better solution
  Iter = iter = 1
end
```

5.3 Differential Evolution

Differential Evolution [40] is a well-established evolutionary algorithm efficient in treating non-linear, non-differentiable and multi-modal objective functions. DE employs three operators, namely: mutation, crossover and selection to develop its population. The steps are briefly described below:

5.3.1 Initialization. The population is randomly initialized within the upper and lower bounds,

$$X_{jk}^{0} = X_{k}^{\min} + rand * \left(X_{k}^{\max} - X_{k}^{\min}\right); \quad j = 1, 2, 3, \ldots, pop; \quad k = 1, 2, 3, \ldots, nv; \quad (20)$$

where pop, nv, respectively denotes the population size and the number of control variables. rand function generates uniform random numbers within the interval [0, 1]. $X_k^{\max}$ and $X_k^{\min}$ respectively denote the upper and lower bounds of the kth control variable.

5.3.2 Mutation. In this phase, random extraction of several individuals from the population and their geometrical manipulation takes place. Mutant vectors $X_j^{/p}$ are created by unsettling a randomly created vector X_a^p with the difference of two other randomly selected vectors X_b^p and X_c^p at pth iteration according to the following equation:

$$X_j^{/p} = X_a^p + F\left(X_b^p - X_c^p\right); \quad j = 1, 2, 3, \ldots, pop.; \quad (21)$$

F denotes the scaling factor and lies in the interval [0, 2]. It controls the perturbation in mutation, thereby improving convergence. Exploration capability is controlled by the population size and the number of individuals extracted randomly in the strategy.

5.3.3 Crossover. In this phase, gene exchange between the individuals takes place. The parent vector (target vector) interacts with the mutated vector and creates a trial vector, which inherits parental genes with some probability. Crossover is represented with the following equation:

$$\left.\begin{aligned} X_{jk}^{//p} &= X_{jk}^{/p} \quad \textit{if rand } k < C_r \textit{ or } k = q \\ &= X_{jk}^{p} \qquad\qquad \textit{otherwise} \end{aligned}\right\} \tag{22}$$

where $j = 1, 2, 3, \ldots, pop$; $k = 1, 2, 3, \ldots, pop$; $X_{jk}^{p}, X_{jk}^{/p}$ and $X_{jk}^{//p}$ denote respectively the kth individual of the jth target vector, mutant vector and trial vector at pth iteration. Randomly chosen index $q \in (k = 1, 2, 3, \ldots, nv)$, ensures that at least one parameter from the mutant vector is taken by it even if the crossover probability C_r is zero. $C_r \in [0, 1]$ helps to maintain diversity of the population so that the algorithm doesn't get trapped into local optima.

5.3.4 Selection. This phase selects the best set amongst the trial vector and the updated target vector by comparing their objective functions. The vector which gives the best value of the objective function (maximum or minimum depending upon the problem), gets selected. The following equation represents the selection procedure:

$$\left.\begin{aligned} X_j^{p+1} &= X_j^{//p} \quad \textit{if } f\left(X_j^{//p}\right) \le f\left(X_j^{p}\right) \\ &= X_j^{p} \qquad\qquad \textit{otherwise} \end{aligned}\right\} \quad j = 1, 2, 3, \ldots, pop. \tag{23}$$

5.3.5 Pseudo- code for DE algorithm.

```
Initialize the population P
Analyse the fitness for each individual of P
while maximum fitness evaluation is not reached
  for j = 1 to pop
    Select uniform vectors randomly a≠b≠c≠j
    k_rand = randint (1, nv)
    for k = 1 to nv
      if rand_k (0, 1) > C_r or k == k_rand
        Y_j(k) = X_a(k) + F(X_b(k) − X_c(k))
      else
        Y_j(k) = X_j(k)
      end
    end
  end
  for j = 1 to nv
  Analyse the offspring Y_j
    if Y_j is better than P_j
    P_j = Y_j
    end
  end
end
```

$X_j(k)$ denotes the kth variable of solution X_j. Y_j denotes the offspring. *randint* (1, *nv*) represents a uniformly distributed random integer between 1 and *nv*. $rand_k$ (0, 1) represents real number randomly distributed in (0, 1). Different DE strategies are available in [40] for the creation of a candidate. Strategy 1 has been discussed here.

5.4 Grey wolf optimizer

GWO is a recently developed meta-heuristic optimization technique, which follows the hunting strategy applied by a grey wolf [41]. Grey wolves live and hunt in a pack of 5–12 members on an average. They are categorized as alpha, beta, delta and omega, whereby alpha is placed at the top level of hierarchy, followed by beta, delta and omega. Their hunting strategy involves tracking the position of prey, chasing, encircling and attacking. The steps are discussed below.

5.4.1 Encircling. The following equation represents encircling behavior of grey wolf:

$$\vec{D} = |\vec{C} \cdot \vec{X}_p(t) - \vec{X}(t)| \tag{24}$$

$$\vec{X}(t+1) = \vec{X}_p(t) - \vec{A} \cdot .\vec{D} \tag{25}$$

where $\vec{D}$ represents a difference vector, t represents the present time. $\vec{A}$ and $\vec{C}$ are coefficient vectors. $\vec{X}$ and $\vec{X}_p$ represent respectively positions of the grey wolf and the prey. Following equations represent the coefficient vectors $\vec{A}$ and $\vec{C}$:

$$\vec{A} = 2 \cdot \vec{a} \cdot \vec{r}_1 - \vec{a} \tag{26}$$

$$\vec{C} = 2 \cdot \vec{r}_2 \tag{27}$$

where $\vec{r}_1$ and $\vec{r}_2$ are random in the interval [0, 1] and components of $\vec{a}$ are linearly decreased from 2 to 0 iteratively. (26) and (27) are used to update position of grey wolves.

5.4.2 Hunting strategy. Alpha guides the hunting process. Beta, delta may participate occasionally in this part. It is assumed that alpha, beta and delta have the best knowledge about the position of the prey in the search space. Following equations represent the overall hunting process:

$$\vec{D}_\alpha = |\vec{C}_1 \cdot \vec{X}_\alpha - \vec{X}| \tag{28}$$

$$\vec{D}_\beta = |\vec{C}_2 \cdot \vec{X}_\beta - \vec{X}| \tag{29}$$

$$\vec{D}_\delta = |\vec{C}_3 \cdot \vec{X}_\delta - \vec{X}| \tag{30}$$

$$\vec{X}_1 = \vec{X}_\alpha - \vec{A}_1 \cdot (\vec{D}_\alpha) \tag{31}$$

$$\vec{X}_2 = \vec{X}_\beta - \vec{A}_2 \cdot (\vec{D}_\beta) \tag{32}$$

$$\vec{X}_3 = \vec{X}_\delta - \vec{A}_3 \cdot (\vec{D}_\delta) \tag{33}$$

$$\vec{X}(t+1) = \frac{\vec{X}_1 + \vec{X}_2 + \vec{X}_3}{3} \tag{34}$$

where $\vec{D}_\alpha$, $\vec{D}_\beta$ and $\vec{D}_\delta$ are respectively the difference vector of alpha, beta and delta. $\vec{X}_1$, $\vec{X}_2$ and $\vec{X}_3$ represent position of the prey with respect to alpha, beta and delta respectively $\vec{X}_\alpha$, $\vec{X}_\beta$, $\vec{X}_\delta$ represent positions of the alpha, beta and delta wolves respectively.

5.4.3 Attacking. The wolves attack and finish the hunt when the prey stops moving. Exploitation capability of GWO technique is governed by vector $\vec{A}$ which is a random number between $[-2a, 2a]$. It allows other search agents to update their position based upon the positions of alpha, beta and delta wolves, and finally attack the prey.

5.4.4 Search for prey. Current position of alpha, beta and delta dictates the search process. Wolves diverge from each other during searching, and converge while attacking the prey. To mathematically model divergence, vector $\vec{A}$ is associated with some random values greater than 1 and less than -1 in order to compel the search agents to diverge from each other. This emphasizes the exploration capability of GWO to search for global optimum value.

5.4.5 Pseudo-code for GWO

```
Initialize the grey wolf population X_i (i = 1, 2, . . . , n).
Initialize a, A and C (coefficient vectors)
Calculate the fitness of each grey wolf.
Find X_α = The best grey wolf (alpha).
Find X_β = The second best grey wolf (beta).
Find X_δ = Third best grey wolf (delta)
  While (iter < maxiter)
    for each grey wolf
      Update the position of the current grey wolf using (34)
    end
    Update a, A and C using (26)
    Calculate the fitness of all grey wolves.
    Update X_α, X_β and X_δ.
    iter = iter + 1;
  end
```

5.5 Collective decision optimization algorithm

Collective decision optimization algorithm (CDO) as described by Zhang et al. [29], is a relatively new metaheuristic algorithm based on the human social behavior influenced by their decision making capabilities. Human beings tend to collect fellows having different capabilities and form a group to arrive at a decision regarding a problem or a solution. Members of the group express as well as exchange ideas and finally select the best idea amongst all. Final decision is influenced by different factors such as: conformity in the members' thinking, experience, leader, viewpoint of other members and innovation.

The terms relating the common evolutionary programs with CDO are as follows:

$$\begin{aligned}&Population = Gathering;\ Population\ size = Total\ members\ present\ in\ the\ meeting\\&or\ deciders;\ Agent = Decider;\ Feasible\ solution = Plans\ or\ ideas;\\&Fitness\ value = plan\ quality;\ Optimal\ solution = bestidea.\end{aligned}$$

The decision making abilities are classified into different phases as follows:

5.5.1 Formation of group. A group of P members is randomly formed within the search space of dimension D as follows:

$$K_i^j = LB^j + rand(0,1) \times \left(UB^j - LB^j\right) \tag{35}$$

where i=1, 2, 3, . . ., P; j=1, 2, 3, . . ., D. *rand* denotes any random number in the interval [0, 1], and LB and UB represents the lower and upper bounds of the control variables.

5.5.2 Experience phase. In a meeting of the group, deciders bring forward their plans based on their personal experiences. In CDO, this is defined as the best position of the agent Φ_A and can be expressed as:

$$\begin{aligned}K_{inew} &= K_i + rand(0,1) \times step\_size \times d_0\\ d_0 &= \Phi_A - K_i\end{aligned} \tag{36}$$

where *rand* is any random number selected from *[0, 1]*, step_size denotes step size for present iteration, and d denotes the direction in which the next decider is selected to share his/her plan.

5.5.3 Others' idea phase. Exchange of ideas between the agents take place in this phase and an agent accepts others' ideas if those are superior to her/his idea. An agent K_j, is selected randomly from the population to exchange idea with K_i. The agent having the better quality plan is selected. This phase is expressed as follows:

$$K_{inew}^{(1)} = K_{inew} + rand(0,1) \times step\_size \times d_1$$
$$d_1 = beta_1 \times d_0 + beta_2 \times (X_j - X_i) \quad (37)$$

where j is the agent selected from the interval *[1, P]*, d_1 is the new direction of movement and $beta_1$ and $beta_2$ are two numbers randomly respectively selected from the intervals *[−1, 1]* and *[0, 2]*.

5.5.4 Group-thinking phase. This phase describes the way agents' decisions are influenced by the direction in which the maximum ideas are inclined to. The position of the group thinking can be assumed to be the geometric center (Φ_G) of each agent. It may be expressed as:

$$\Phi_G = \frac{1}{P}(K_1, K_2, \ldots, K_P) \quad (38)$$

The updated position of the agent is calculated as:

$$newK_i^{(2)} = newK_i^{(1)} + rand(0,\ 1) \times step\_size \times d_2$$
$$d_2 = beta_1 \times d_1 + beta_2 \times (\Phi_G - K_i) \quad (39)$$

where d_2 is the new direction in which the agents ideas progresses.

5.5.5 Leader phase. Overall decision is made under the influence of the leader who decides the direction of movement and final output. Mathematically it can be represented as:

$$newK_i^{(3)} = newK_i^{(2)} + rand(0,\ 1) \times step\_size \times d_3$$
$$d_3 = beta_1 \times d_2 + beta_2 \times (\Phi_L - K_i) \quad (40)$$

where d_3 is the new direction in which the agents ideas progresses. Leader (Φ_L) is the best agent in the meeting.

The leader has the power to change his/her idea by himself/herself. Random walk strategy is used by this algorithm for local search.

$$newK_p = \Phi_L + W_p \ (p = 1,\ 2,\ 3,\ 4,\ 5) \quad (41)$$

where W_p is any vector randomly selected from within the interval [0, 1].

5.5.6 Innovation phase. Innovation refers to the process involved in improving the decision making process. This is achieved by making small perturbation in the existing variables (mutation factors) and can be implemented as:

$$rand1 \leq M$$
$$newK_i^{(4)} = newK_i^{(4)} \quad (42)$$
$$newK_i^{(4,F)} = LB(F) + rand2 \times (UB(F) - LB(F))$$

where *rand1* and *rand2* are two uniformly distributed random numbers within *[0, 1]*, F is randomly generated within interval [1, D], M denotes mutation factor used to avoid premature convergence.

Proper selection of the *step_size* plays an important part in deciding exploration and exploitation of the population. Larger valued *step_size* in the initial stages ensure better exploration and smaller values in the later parts ensure proper exploitation of the population. An adaptive mechanism used by the algorithm is described below:

$$step\_size(t) = 2 - 1.7\left(\frac{t-1}{T-1}\right) \quad (43)$$

where t denotes the present iteration and T denotes the maximum iteration number.

5.5.7 Pseudo-code for CDO

```
Initialize group members (also known as agents, those who will
   take part in the meeting) for the meeting (Pop) and
   termination criterion (maxiter)
Calculate the fitness of each group member, identify leader
while termination criterion is not satisfied (iter ≤ maxiter)
Find the global best solution (Φ_L)
Compute the step size (stepsize(t)) using (43)
for i = 1: N            ; N being the population size
   newpop = []
   if fitness = bestfitness (Φ_L)
         Calculate the new solutions (newKp) by Eq. (41)
         newpop = newKp
      else
         Change the location of member by (36)–(40), and (43);
   and calculate
         K_inew, K_inew^(1), newK_i^(2), newK_i^(3), newK_i^(4,F)
         newpop = [K_inew, K_inew^(1), newK_i^(2), newK_i^(3), newK_i^(4,F)]
      end
      Analyze fitness of newpop
      Update K_i and pbest (personal best position) from the
   resultant positions
   end
   iter = iter + 1
end
Output best solution
```

Steps involved in parameter tuning of PSS using CDO are as follows:

Step 1: Randomly initialize a group of P members within the search space having dimension D. Set the members i.e., control parameters (PSS gain and lead-lag time constant) of the group within their upper and lower bounds based on (11). Choose maximum fitness evaluation (maxFE).

Step 2: Analyze small signal stability of the system for each member of the group and obtain eigenvalues and check whether they satisfy the inequality constraints of (11).

Step 3: Determine the plan quality (fitness function) as per (9) for each group, which is eigenvalue based. Store total number of fitness evaluation within the variable FE.

Step 4: Identify the new best position of agents (K_{inew}) from the population, based on their quality of plan (fitness values). This forms the modified group set.

Step 5: Update the population of groups as per the different phases of CDO employing (36)–(42).

Step 6: Find the best plan and best group. Best plan is the minimum of the fitness function evaluated for each solution set and best group is the solution set which gives the best plan.

Step 7: Go to step 5 and repeat until value of FE reaches the predefined maxFE.

6. Results and discussion

The purpose of this section is to analyze system performances with the help of a newly proposed algorithm. To show the application and superiority of CDO, two test systems are considered and mentioned in the earlier Section 2. First one is WSCC 3 machine 9 bus system and second one is IEEE 14 bus system.

6.1 Results regarding PSS parameters tuning

Eigenvalues obtained using CDO are used to determine stability of the system and are compared with those achieved by GWO, DE, WOA and CSA. Results demonstrate supremacy of CDO over GWO and CSA in assessing small signal stability of the system. To show the effectiveness of the proposed algorithm in mitigating low frequency oscillations, PSS were installed in all the machines for both test systems. System eigenvalues and damping ratios of electromechanical mode are shown in Tables 3 and 4 respectively, when both systems are subjected to different loading conditions. Even though PSS is for improving the damping torque primarily, during the disturbances it is expected to make slight contribution to synchronizing torque enhancement, also during post disturbance the synchronizing torque

	Light load	Normal load	High load
No stabilizer	−1.43600 ± 13.275i, 0.10755	−0.90694 ± 13.576i, 0.06666	−0.79932 ± 13.633i, 0.05853
	−0.37734 ± 9.1310i, 0.04129	−0.18488 ± 9.0462i, 0.02043	−0.16828 ± 8.7924i, 0.01914
CSA PSS	−1.82340 ± 13.247i, 0.13636	−1.30310 ± 13.533i, 0.09585	−1.13930 ± 13.593i, 0.08352
	−1.15910 ± 9.2183i, 0.12476	−1.08450 ± 9.0885i, 0.11849	−1.20850 ± 8.8804i, 0.13484
WOA PSS	−1.83560 ± 13.239i, 0.13730	−1.32500 ± 13.563i, 0.09720	−1.20850 ± 14.164i, 0.08500
	−1.14360 ± 9.0870i, 0.12490	−1.12500 ± 10.234i, 0.10930	−1.52640 ± 9.5460i, 0.15790
DE PSS	−2.05600 ± 13.567i, 0.14980	−1.28900 ± 13.345i, 0.09610	−1.34500 ± 14.165i, 0.09450
	−1.20100 ± 9.3450i, 0.12750	−1.21000 ± 10.548i, 0.11400	−1.98450 ± 9.3298i, 0.20730
GWO PSS	−1.90820 ± 13.453i, 0.14044	−1.42740 ± 13.743i, 0.10331	−1.24250 ± 13.774i, 0.08984
	−1.29170 ± 9.7794i, 0.13095	−1.15540 ± 9.8455i, 0.11655	−2.46510 ± 8.8214i, 0.26913
CDO PSS	−2.37830 ± 13.389i, 0.17489	−1.84620 ± 13.592i, 0.13459	−1.56610 ± 13.578i, 0.11458
	−1.77680 ± 9.8859i, 0.17690	−1.95210 ± 9.7341i, 0.19663	−2.07950 ± 9.5543i, 0.21267

Table 3. Electromechanical modes and damping ratios for WSCC 3 machine 9 bus system.

	Light load	Normal load	High load
No stabilizer	−1.2003 ± 12.253i, 0.097493	−1.1890 ± 12.050i, 0.098195	−1.1796 ± 11.766i, 0.099755
	−2.7730 ± 9.7799i, 0.272790	−2.7507 ± 9.7174i, 0.272370	−2.7175 ± 9.6111i, 0.272080
	−0.7398 ± 10.671i, 0.069159	−0.7313 ± 10.682i, 0.068298	−0.7064 ± 10.666i, 0.066083
	−0.8589 ± 9.5242i, 0.089816	−0.8027 ± 9.4623i, 0.084523	−0.7355 ± 9.3467i, 0.078448
CSA PSS	−3.3240 ± 8.1049i, 0.37945	−3.7132 ± 8.6628i, 0.39397	−3.3451 ± 8.7049i, 0.35870
	−2.3269 ± 7.9262i, 0.28168	−2.4751 ± 8.0025i, 0.29548	−2.9269 ± 8.9262i, 0.68204
	−2.0684 ± 11.863i, 0.17177	−1.9798 ± 11.856i, 0.16471	−2.0684 ± 11.863i, 0.17177
	−1.2044 ± 10.139i, 0.11796	−1.2070 ± 10.149i, 0.11810	−1.2044 ± 10.139i, 0.11796
WOA PSS	−3.7840 ± 8.9742i, 0.38853	−4.129 ± 8.61290i, 0.43229	−4.3210 ± 8.9742i, 0.43382
	−2.5345 ± 7.5388i, 0.31867	−2.7834 ± 7.7717i, 0.33717	−2.5340 ± 7.1988i, 0.33203
	−2.5745 ± 11.650i, 0.21578	−2.4845 ± 11.676i, 0.20813	−2.5745 ± 11.650i, 0.21578
	−1.0245 ± 9.9000i, 0.10294	−1.0412 ± 9.9213i, 0.10437	−1.0245 ± 9.9000i, 0.10294
DE PSS	−4.9435 ± 8.9077i, 0.48525	−5.0835 ± 9.0329i, 0.49044	−4.9435 ± 8.9077i, 0.48525
	−3.4404 ± 8.2963i, 0.38306	−3.4798 ± 8.3972i, 0.38283	−3.4404 ± 8.2963i, 0.38306
	−3.9331 ± 10.129i, 0.36197	−3.7253 ± 10.479i, 0.33496	−3.9331 ± 10.129i, 0.36197
	−1.0328 ± 9.5096i, 0.10797	−1.0121 ± 9.5751i, 0.10512	−1.0328 ± 9.5096i, 0.10797
GWO PSS	−5.1465 ± 7.5119i, 0.56519	−5.2455 ± 7.4778i, 0.57427	−5.1465 ± 7.5119i, 0.56519
	−4.6937 ± 11.095i, 0.38962	−4.6286 ± 11.300i, 0.37904	−4.6937 ± 11.095i, 0.38962
	−1.5901 ± 12.192i, 0.12933	−1.4915 ± 12.228i, 0.12108	−1.5901 ± 12.192i, 0.12933
	−1.5868 ± 8.0461i, 0.19349	−1.5595 ± 8.1410i, 0.18814	−1.3868 ± 8.0462i, 0.16985
CDO PSS	−7.0070 ± 7.8545i, 0.66570	−7.3189 ± 7.6198i, 0.69272	−7.0070 ± 7.8545i, 0.66570
	−4.7360 ± 7.9699i, 0.51085	−4.8228 ± 8.0955i, 0.51180	−4.7360 ± 7.9699i, 0.51085
	−5.2410 ± 11.890i, 0.40334	−5.2440 ± 11.909i, 0.40300	−5.2410 ± 11.890i, 0.40334
	−4.0692 ± 10.336i, 0.36633	−4.0529 ± 10.618i, 0.35661	−4.0692 ± 10.336i, 0.36633

Table 4. Electromechanical modes and damping ratios for IEEE 14 bus system.

contribution should be slightly positive apart from its main and substantial positive damping torque contribution. Therefore, all these means imaginary part of electromechanical modes should slightly increase.

It is very much clear from the above table that CDO is able to shift all real parts of electromechanical modes towards left half of *S* plane having enhanced damping ratios under

		CSA	WOA	DE	GWO	CDO
Generator1	*Kpss*	17.07600	5.017000	11.08400	11.84100	2.569100
	T1 (s)	0.238070	0.100000	0.134700	1.034500	1.252700
	T2 (s)	0.010523	0.052334	0.028844	0.017099	0.071439
	T3 (s)	0.346370	1.410500	0.983990	0.926750	1.291200
	T4 (s)	0.063216	0.029970	0.139400	0.119170	0.117900
Generator2	*Kpss*	1.339800	11.89800	1.957700	1.931500	1.917600
	T1 (s)	1.245200	0.335300	0.327970	0.267260	0.569380
	T2 (s)	0.010000	0.010000	0.026173	0.016836	0.027684
	T3 (s)	0.386820	0.245860	1.404600	1.500000	1.147500
	T4 (s)	0.010000	0.029061	0.010391	0.010000	0.025351
Generator3	*Kpss*	2.376200	4.329900	4.599500	3.991800	6.316000
	T1 (s)	0.100000	0.373800	0.931190	0.160110	0.188030
	T2 (s)	0.052728	0.119430	0.082403	0.088431	0.131070
	T3 (s)	0.100000	0.100000	0.100000	0.169610	0.206240
	T4 (s)	0.046983	0.120820	0.044372	0.030897	0.150000
Simulation time (s)		31.49850	30.51320	28.21950	25.46820	21.41550

Table 5.
Tuned PSS parameters for various algorithms for WSCC 3 machine 9 bus system.

		CSA	WOA	DE	GWO	CDO
Generator1	*Kpss*	4.132000	4.341400	8.152700	5.791300	4.630100
	T1 (s)	0.100000	0.101560	1.338900	0.681330	0.114800
	T2 (s)	0.046901	0.040558	0.010000	0.036983	0.050230
	T3 (s)	1.500000	1.386900	0.100000	0.262250	1.306500
	T4 (s)	0.010000	0.015280	0.010000	0.035294	0.020977
Generator2	*Kpss*	4.012100	2.405900	17.66600	16.38100	43.38400
	T1 (s)	1.086200	1.058800	0.297860	0.517430	1.326600
	T2 (s)	0.087176	0.101770	0.010000	0.044588	0.150000
	T3 (s)	0.866110	1.065200	0.170540	1.282100	0.167960
	T4 (s)	0.137770	0.077238	0.010000	0.064138	0.143540
Generator3	*Kpss*	34.25100	32.00400	4.885900	26.79100	48.94900
	T1 (s)	1.216600	1.500000	0.713230	1.235700	0.397110
	T2 (s)	0.039207	0.036996	0.052578	0.119860	0.066386
	T3 (s)	0.150150	0.149710	0.265630	0.156280	0.144350
	T4 (s)	0.024825	0.015512	0.074015	0.105860	0.115220
Generator4	*Kpss*	21.52800	22.09600	50.00000	30.51800	19.50700
	T1 (s)	1.127600	0.688850	0.508050	1.250400	0.289100
	T2 (s)	0.108970	0.101430	0.010000	0.114200	0.043982
	T3 (s)	0.151170	0.255610	0.249730	0.104030	1.453000
	T4 (s)	0.083815	0.083591	0.150000	0.074985	0.082137
Generator5	*Kpss*	30.56200	30.51300	23.40200	40.91000	49.94000
	T1 (s)	0.223230	0.204670	0.984220	0.350090	0.274500
	T2 (s)	0.150000	0.150000	0.021779	0.034848	0.098783
	T3 (s)	1.226700	1.078100	0.100000	1.218700	1.491300
	T4 (s)	0.114320	0.115730	0.100000	0.069048	0.113400
Simulation time (s)		35.58670	32.95680	30.45380	28.95060	25.12340

Table 6.
Tuned PSS parameters for various algorithms in case of IEEE 14 bus system.

light, normal and heavy loading conditions as compared to other techniques. To show the robustness of the proposed design, PSS parameters are tuned for a single operating point i.e., the best group for that point is obtained. Then, all operating points are analyzed for this group and their responses are obtained. For each operating condition CDO provides robust performance and achieves better damping characteristics as compared to GWO, DE, WOA and CSA based PSS. The set values for the PSS parameters for different algorithms are listed in (Tables 5 and 6) respectively for both the test systems.

All the simulations have been done using MATLAB software. A population size of **50** has been considered in all cases and convergences of the algorithms have been studied for 100 iterations. Figure 5. Represents the convergence characteristics for both WSCC 3 machine 9

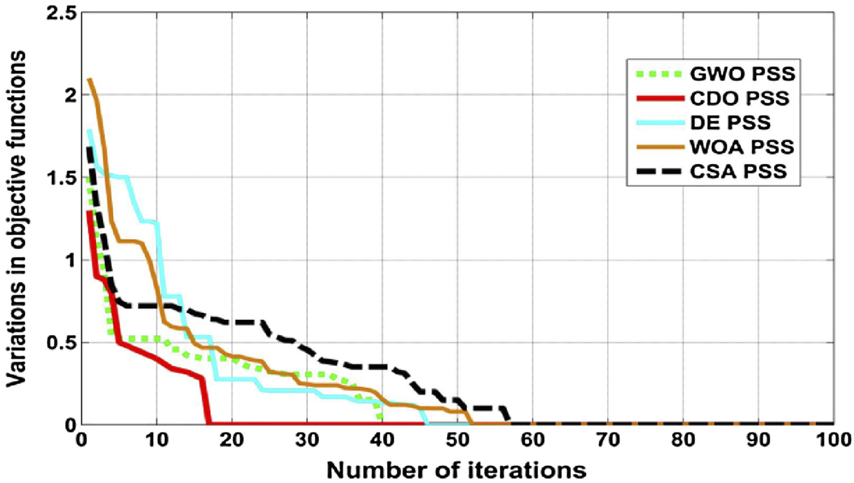

(a) Convergence Characteristics for WSCC 3 machines 9 bus system.

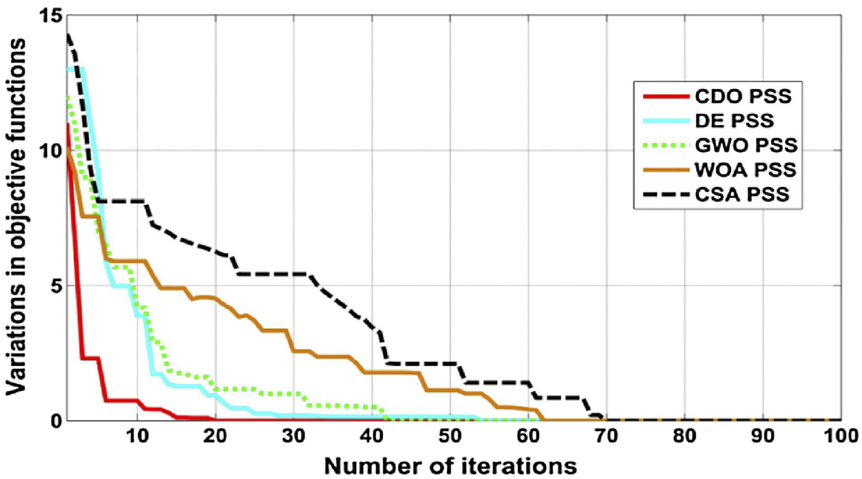

(b) Convergence Characteristics for IEEE 14 bus system

Figure 5.
Variations in objective functions.

bus and IEEE 14 bus system respectively. It shows decreasing objective function in each iteration for all the optimization techniques which finally settles down to zero (I = 0). This indicates that all electromechanical modes have entered into the D-space in the negative half of s-plane. Also, CDO converges faster (16 iterations for first test system and 20 for second one) as compared to GWO (40 iteration for 9 bus system 42 for IEEE 14 bus), DE (45 iterations for 9 bus 54 for IEEE 14 bus system), WOA (52 and 62 respectively) and CSA (57 and 70 iterations respectively).

6.2 Results regarding PSS location

As PSSs are very expensive, it is not wise to install PSS in all the generators. CDO is applied in this paper to find out optimal locations for PSS. Additionally it is also required to maximize

Table 7. PSS settings and locations set obtained for WSCC 3 machine 9 bus system.

With CDO algorithm					
No. PSS	PSS set	G_1	G_2	G_3	Damping ratio
1 PSS	*Kpss*			11.52410	0.065809
	T1 (s)			0.301562	
	T2 (s)			0.010000	
	T3 (s)			0.419568	
	T4 (s)			0.010000	
2 PSS	*Kpss*		3.096100	4.126400	0.167550
	T1 (s)		0.674120	0.130090	
	T2 (s)		0.020884	0.069851	
	T3 (s)		0.597990	0.202520	
	T4 (s)		0.010000	0.092616	
3 PSS	*Kpss*	2.569100	1.917600	6.316000	0.174890
	T1 (s)	1.252700	0.569380	0.188030	
	T2 (s)	0.071439	0.027684	0.131070	
	T3 (s)	1.291200	1.147500	0.206240	
	T4 (s)	0.117900	0.025351	0.150000	

Table 8. PSS settings and locations set obtained for IEEE 14 bus system.

No. PSS	PSS set	G_1	G_2	G_3	G_4	G_5	Damping ratio
2 PSS	*Kpss*			5.980200		27.62800	0.097259
	T1 (s)			0.103650		1.339300	
	T2 (s)			0.451010		0.013734	
	T3 (s)			0.101470		0.829560	
	T4 (s)			0.117730		0.113180	
3 PSS	*Kpss*			42.40910	14.36160	9.101760	0.110383
	T1 (s)			0.100792	0.620330	0.923394	
	T2 (s)			0.135107	0.069186	0.148245	
	T3 (s)			1.008670	0.527537	0.333954	
	T4 (s)			0.013524	0.127541	0.076324	
4 PSS	*Kpss*	4.975100		20.47500	13.59100	44.49700	0.303640
	T1 (s)	0.608230		1.017200	1.302800	0.491490	
	T2 (s)	0.023022		0.092357	0.029223	0.122930	
	T3 (s)	0.327650		0.194900	0.804570	0.856790	
	T4 (s)	0.053213		0.129930	0.098747	0.135250	
5 PSS	*Kpss*	4.630100	43.38400	48.94900	19.50700	49.94000	0.366330
	T1 (s)	0.114800	1.326600	0.397110	0.289100	0.274500	
	T2 (s)	0.050230	0.150000	0.066386	0.043982	0.098783	
	T3 (s)	1.306500	0.167960	0.144350	1.453000	1.491300	
	T4 (s)	0.020977	0.143540	0.115220	0.082137	0.113400	

the damping ratio and minimize the real parts of the electro-mechanical modes, subjected to various combinations of PSS. To provide acceptable damping to the system as well as to make it stable, minimum one PSS is considered for the first test system and two for the second one. Number of available PSS is assumed as 1, 2 and 3 for the first test system and 2, 3, 4, 5 for second one respectively. Now by using (9) and applying CDO technique, the optimal location of PSS is found out for both the test systems and are tabulated in (Tables 7 and 8) respectively.

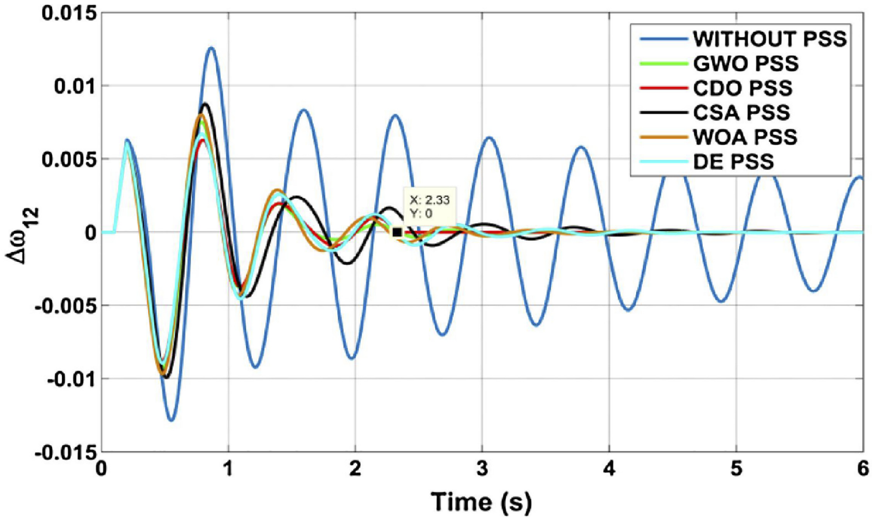

(a) Changes in $\Delta\omega_{12}$.

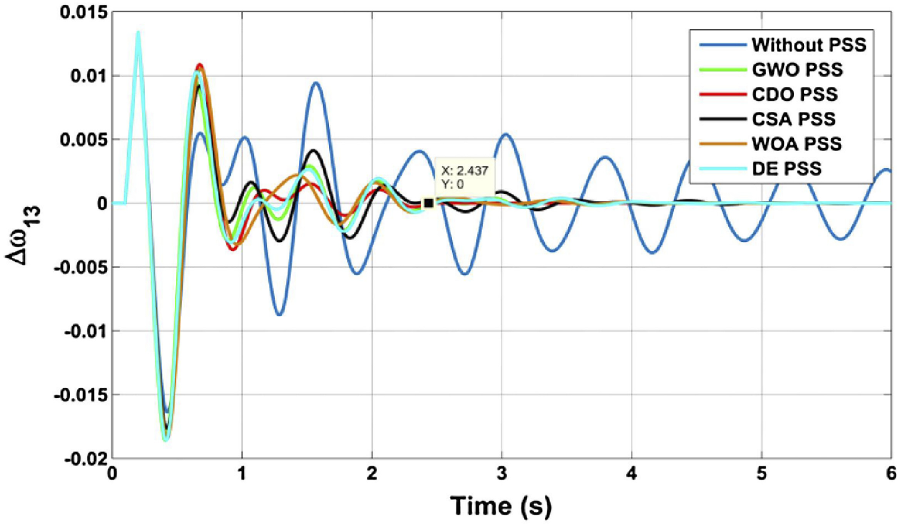

(b) Changes in $\Delta\omega_{13}$.

Figure 6.
Speed deviations for normal load (WSCC 3 machine 9 bus system).

For the first case it can be observed from Table 7, that G_1, G_2 and G_3 are the optimal locations for installing three PSS, whereas for two PSS case, Generator G_2, G_3 are the optimal locations. In case of single PSS installation, generator G_3 is obtained as optimal location. For all the optimal locations, the tuned values of PSS parameters and the least damping rations are summarized in the above table. The minimum damping ratio is 0.065809 in case of one PSS and increases to 0.16755 when two PSS are installed in two generators. This damping ratio further increased to 0.17489 when PSS are installed in all three generators. When two PSSs are installed in the

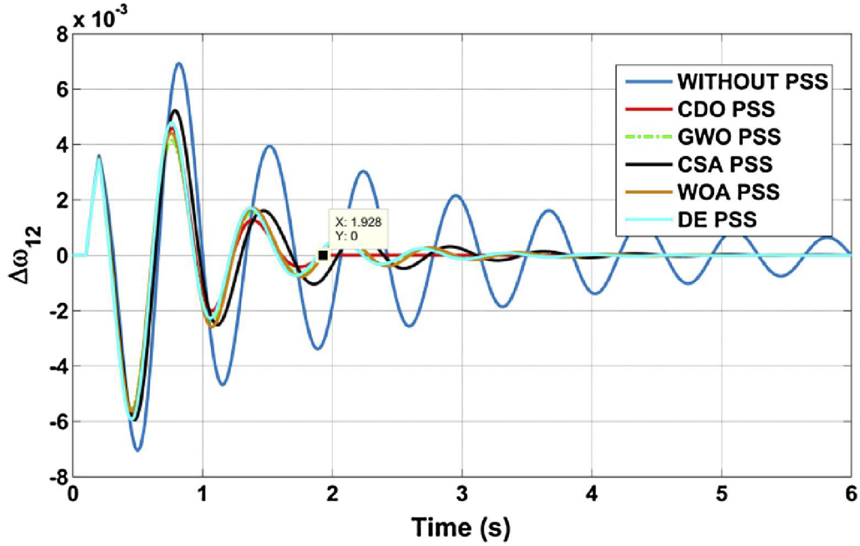

(a) Changes in $\Delta\omega_{12}$.

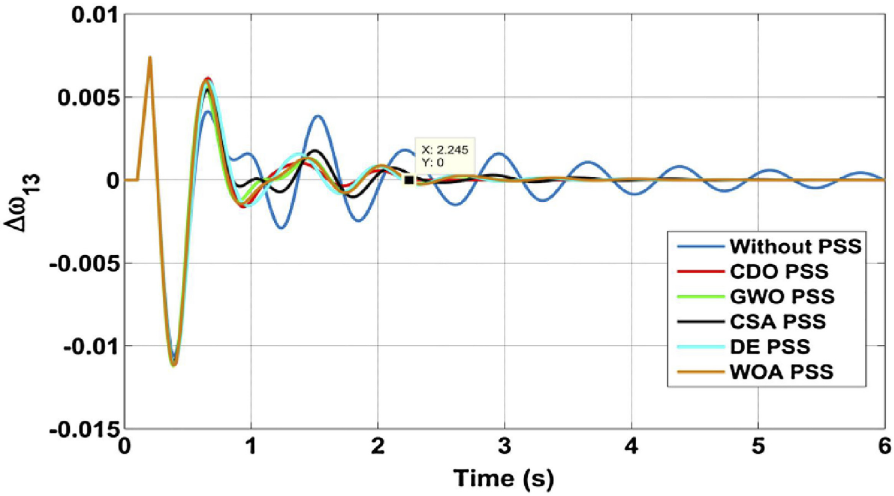

(b) Changes in $\Delta\omega_{13}$.

Figure 7.
Speed deviations for light load (WSCC 3 machine 9 bus system).

system, significant improvement in damping ratios are observed as compared to the case when single PSS is installed. Also there cannot be seen any huge differences when three PSSs are installed. Therefore installing two PSSs in the system provides sufficient damping to low frequency oscillations and as a conclusion G_2, G_3 may be considered as optimal locations.

Similarly, for the second test system it has been found from Table 8, that in case of four generators case, G_1, G_3, G_4, G_5 combination is found to be optimal, whereas G_1, G_3, G_4 and G_3,

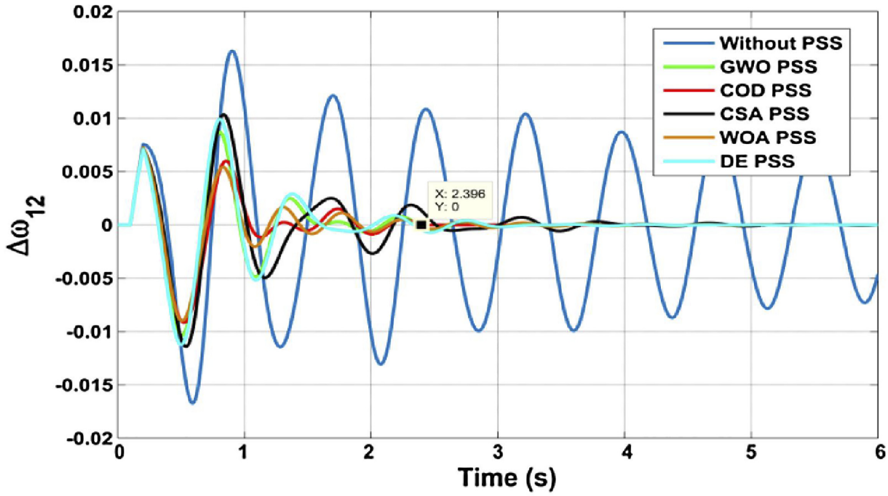

(a) Changes in $\Delta\omega_{12}$ for heavy load.

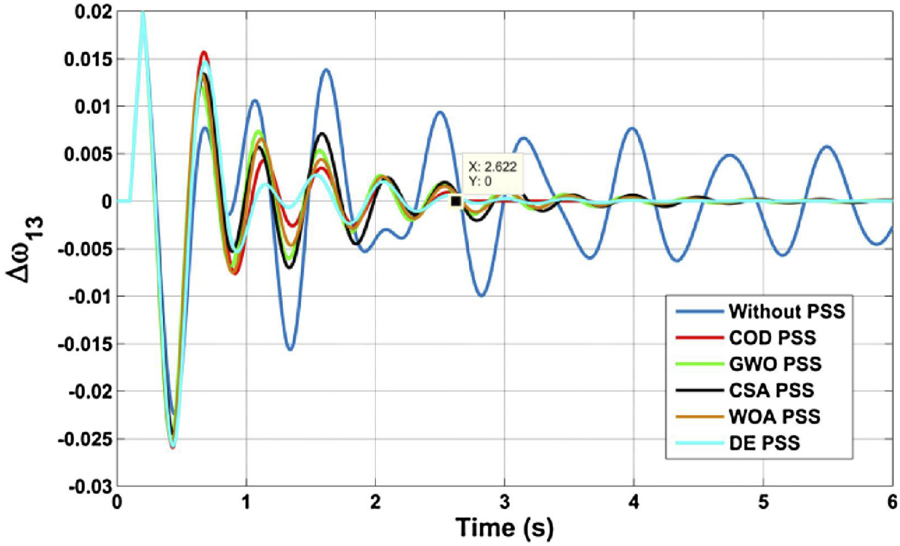

(b) Changes in $\Delta\omega_{13}$.

Figure 8.
Speed deviations for heavy load (WSCC 3 machine 9 bus system).

G_2 are the best combinations in case of three PSS and two PSS respectively. It is observed that in case of four PSS i.e., G_1, G_3, G_4, G_5 combination provides an acceptable damping to the system to maintain its stability. So, for second test system, G_1, G_3, G_4, G_5 combination may be considered as the optimal location.

6.3 Response of the system under different loading conditions

For validation of the proposed algorithm some time domain simulations have been done for both WSCC 3 machine 9 bus and IEEE 14 bus systems when subjected to different loading conditions as well as for faulted condition.

6.3.1 Responses for WSCC 3 machine 9 bus system. A three phase fault is applied near bus 7 at time 0.1 s and cleared at 0.2 s (fault clearing time) and responses are obtained for lightly loaded, normally loaded and heavily loaded conditions.

Figure 6 shows responses of $\Delta\omega_{12}$, $\Delta\omega_{13}$ during severe fault under normal loading conditions obtained by each of the algorithms mentioned above. It can be observed that the newly proposed CDO is more stabilized than other optimization techniques and requires mean settling time of 2.4 s to mitigate the system oscillations, whereas GWO, DE, WOA and CSA requires more time to settle down.

Figure 7 shows response of the system under lightly loaded conditions and it can be seen clearly that CDO provides adequate damping to the oscillatory modes and also reduces the mean settling time to 2.1 s which is lesser than other optimizing techniques.

Figure 8 shows response of the system under heavy loaded conditions. Similarly mean settling times for CDO is 2.5 s whereas GWO and CSA take more time to settle down. Therefore it can be concluded that in every case CDO designed PSS gives better performance and is able to provide sufficient damping to the system to mitigate low frequency oscillations.

It is observed from Figures 6(a), 7(a), 8(a) that first swing has a steeper peak, and the second peak is bigger than the first swing. To demonstrate this, response of electrical power output varying with time for each machine is plotted under heavily loaded condition for no PSS installed in it. From Figure 9. it is clear that the peak of P_{e2} in the second swing is lesser than first one. So, there will be more acceleration and that is the reason machine has less

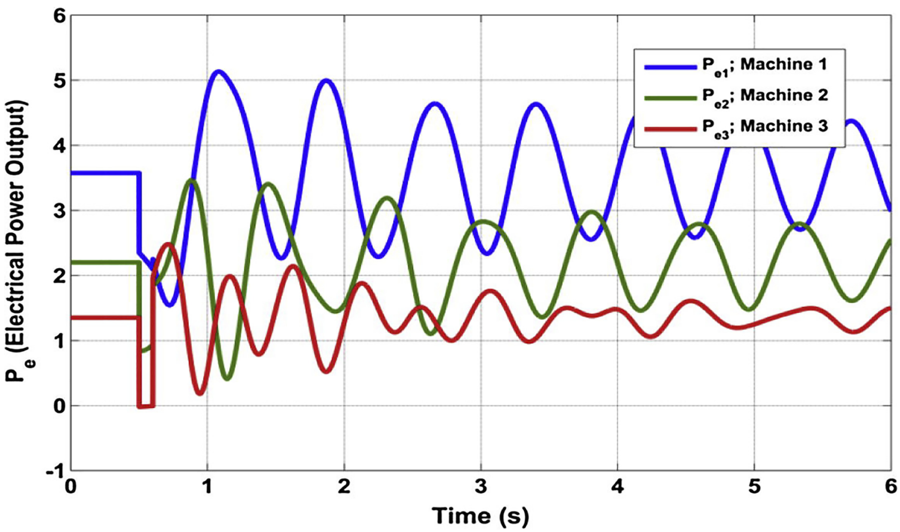

Figure 9.
Electrical Output (Pe) under heavy load when PSS is not installed (WSCC 3 machine 9 bus system).

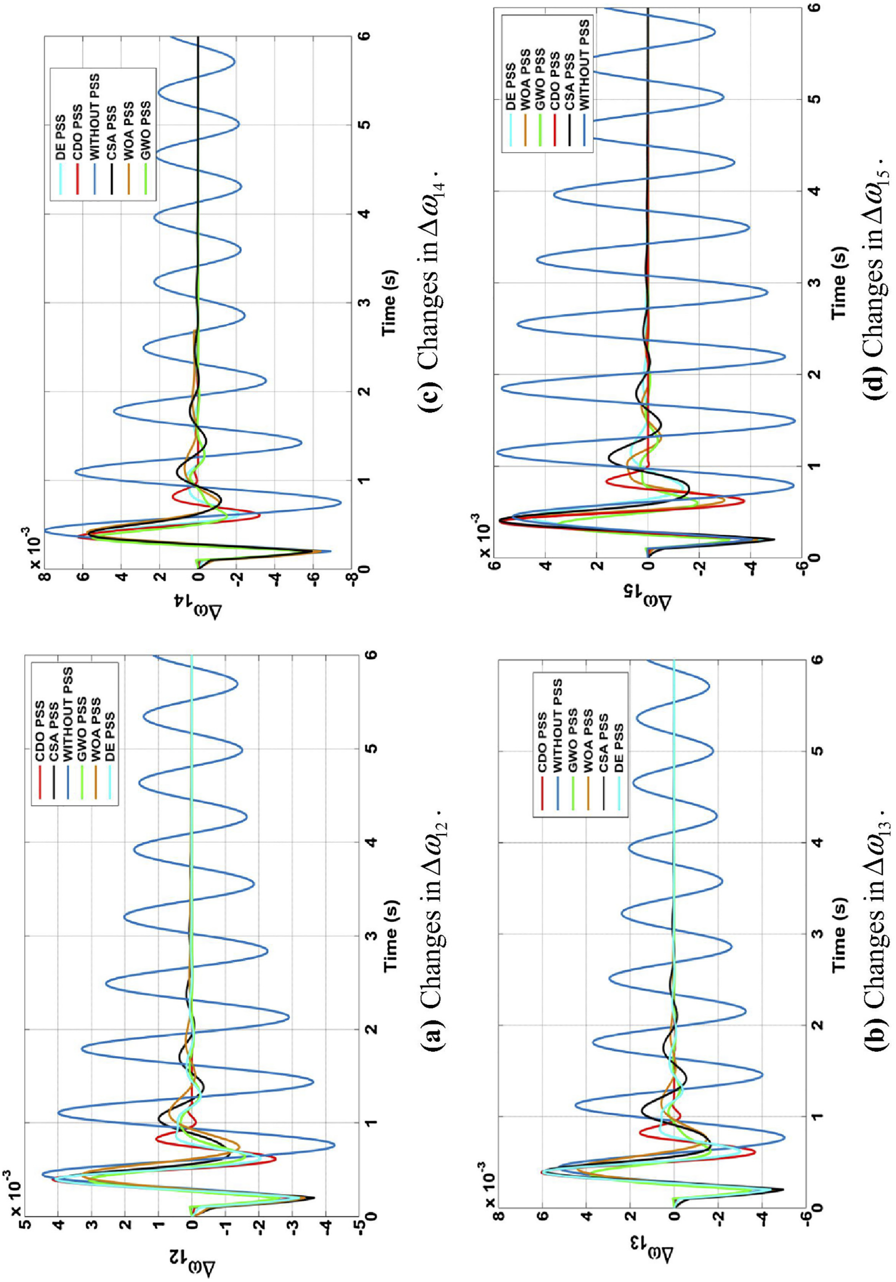

(a) Changes in $\Delta\omega_{12}$.

(b) Changes in $\Delta\omega_{13}$.

(c) Changes in $\Delta\omega_{14}$.

(d) Changes in $\Delta\omega_{15}$.

Figure 10.
Speed deviations for light load (IEEE 14 bus system).

synchronizing strength in the second swing, giving higher peak. Similar explanation will be applicable for light load and normal load conditions.

6.3.2 Responses for IEEE 14 bus system. Performance of CDO has been analyzed for different cases and comparison of results with those of other algorithms demonstrates its efficiency in enhancing overall system stability. In order to assess the capability of CDO in handling a larger and complex system, it has also been applied to IEEE 14 bus test system. The system is tested under all conditions studied for WSCC 3 machine 9 bus systems. A three phase fault is applied near bus 10 at time 0.1 s and cleared at 0.2 s (fault clearing time) and responses are observed. Every possible scenario for obtaining speed deviation curves have been tried out, but for the sake of brevity, few of the responses are shown in this paper. From the plots obtained, Figure 10 it can be observed that CDO based PSS achieved the lowest settling time as compared to other algorithms which means better damping and enhance better stability of the system.

7. Conclusion

New metaheuristic optimization techniques, CDO, GWO, DE, WOA and CSA have been presented in this paper for the optimal design of CPSS. Best tuned parameter set for the PSS are obtained for CDO. It is observed that damping ratios of the weakly damped oscillatory modes have improved after the addition of PSS, thereby enhancing the dynamic performance of system stability greatly. Simulated results established CDO's superiority over GWO, DE, WOA and CSA optimization techniques. The robustness of the designed PSS controller for damping out oscillations under different operating conditions is also established. Application of the designed controller in large-scale multi area power system network under different fault conditions may be done in the future.

References

[1] G. Rogers, Power System Oscillations, Springer Science & Business Media, 2012.

[2] G.J. Dudgeon, W.E. Leithead, A. Dysko, J. o'Reilly, J.R. McDonald, The effective role of AVR and PSS in power systems: frequency response analysis, IEEE Trans. Power Syst. 22 (4) (2007) 1986–1994.

[3] P.W. Sauer, M.A. Pai, J.H. Chow, Power System Dynamics and Stability: With Synchrophasor Measurement and Power System Toolbox, John Wiley & Sons, 2017.

[4] G.N. Taranto, J.H. Chow, A robust frequency domain optimization technique for tuning series compensation damping controllers, IEEE Trans. Power Syst. 10 (3) (1995 Aug) 1219–1225.

[5] H. Werner, P. Korba, T.C. Yang, Robust tuning of power system stabilizers using LMI-techniques, IEEE Trans. Contr. Syst. Technol. 11 (1) (2003 Jan) 147–152.

[6] M.A. Abido, Pole placement technique for PSS and TCSC-based stabilizer design using simulated annealing, Int. J. Electr. Power Energy Syst. 22 (8) (2000) 543–554.

[7] M. Eslami, H. Shareef, A. Mohamed, Application of artificial intelligent techniques in PSS design: a survey of the state-of-the-art methods, Przegląd Elektrotechniczny (Electr. Rev.) 87 (4) (2011).

[8] Y. Zhang, *et al.*, An artificial neural network based adaptive power system stabilizer, IEEE Trans. Energy Convers. 8 (1) (1993) 71–77.

[9] A. Mahabuba, M. Abdullah Khan, Small signal stability enhancement of a multi-machine power system using robust and adaptive fuzzy neural network-based power system stabilizer, Int. Trans. Electr. Energy Syst. 19 (7) (2009) 978–1001.

[10] R. Segal, A. Sharma, M.L. Kothari, A self-tuning power system stabilizer based on artificial neural network, Int. J. Electr. Power Energy Syst. 26 (6) (2004) 423–430.

[11] L.H. Hassan, M. Moghavvemi, H.A. Mohamed, Power system stabilization based on artificial intelligent techniques; a review, in: International Conference for Technical Postgraduates (TECHPOS), 2009, IEEE, 2009, pp. 1–6.

[12] M.A. Abido, Y.L. Abdel-Magid, A genetic-based fuzzy logic power system stabilizer for multimachine power systems, in: IEEE International Conference on Systems, Man, and Cybernetics, 1997, Computational Cybernetics and Simulation, 1997, IEEE, 1997, pp. 329–334.

[13] M.J. Bosco, A.D.J. Raju, Power system stabilizer using fuzzy logic controller in multimachine power systems (2007), http://dx.doi.org/10.1049/ic:20070599.

[14] P. Hoang, K. Tomsovic, Design and analysis of an adaptive fuzzy power system stabilizer, IEEE Trans. Energy Convers. 11 (2) (1996) 455–461.

[15] Z.Y. Dong, Y.V. Makarov, D.J. Hill, Genetic algorithms in power system small signal stability analysis (1997), http://dx.doi.org/10.1049/cp:19971857.

[16] P. Zhang, A.H. Coonick, Coordinated synthesis of PSS parameters in multi-machine power systems using the method of inequalities applied to genetic algorithms, IEEE Trans. Power Syst. 15 (2) (2000) 811–816.

[17] A. Stativă, M. Gavrilaş, V. Stahie, Optimal tuning and placement of power system stabilizer using particle swarm optimization algorithm, in: International Conference and Exposition on Electrical and Power Engineering (EPE) 2012, IEEE, 2012, pp. 242–247.

[18] A. Safari, A PSO procedure for a coordinated tuning of power system stabilizers for multiple operating conditions, J. Appl. Res. Technol. 11 (5) (2013) 665–673.

[19] H.E. Mostafa, M.A. El-Sharkawy, A.A. Emary, K. Yassin, Design and allocation of power system stabilizers using the particle swarm optimization technique for an interconnected power system, Int. J. Electr. Power Energy Syst. 34 (1) (2012) 57–65.

[20] S. Panda, Robust coordinated design of multiple and multi-type damping controller using differential evolution algorithm, Int. J. Electr. Power Energy Syst. 33 (4) (2011) 1018–1030.

[21] S. Panda, Differential evolutionary algorithm for TCSC-based controller design, Simul. Model. Pract. Theory 17 (10) (2009) 1618–1634.

[22] A. Ameli, M. Farrokhifard, A. Ahmadifar, A. Safari, H.A. Shayanfar, Optimal tuning of power system stabilizers in a multi-machine system using firefly algorithm, in: 12th International Conference on Environment and Electrical Engineering (EEEIC), 2013, IEEE, 2013, pp. 461–466.

[23] S.A. Elazim, E.S. Ali, Optimal power system stabilizers design via cuckoo search algorithm, Int. J. Electr. Power Energy Syst. 75 (2016) 99–107.

[24] M.A. Abido, Y.L. Abdel-Magid, Optimal design of power system stabilizers using evolutionary programming, IEEE Trans. Energy Convers. 17 (4) (2002) 429–436.

[25] M.A. Abido, A novel approach to conventional power system stabilizer design using tabu search, Int. J. Electr. Power Energy Syst. 21 (6) (1999) 443–454.

[26] M.A. Abido, Robust design of multimachine power system stabilizers using simulated annealing, IEEE Trans. Energy Convers. 15 (3) (2000) 297–304.

[27] D.K. Sambariya, R. Prasad, Robust tuning of power system stabilizer for small signal stability enhancement using metaheuristic bat algorithm, Int. J. Electr. Power Energy Syst. 61 (2014) 229–238.

[28] S. Mishra, M. Tripathy, J. Nanda, Multi-machine power system stabilizer design by rule based bacteria foraging, Electr. Power Syst. Res. 77 (12) (2007) 1595–1607.

[29] Q. Zhang, R. Wang, J. Yang, K. Ding, Y. Li, J. Hu, Collective decision optimization algorithm: a new heuristic optimization method, Neurocomputing 221 (2017) 123–137.

[30] M.A. Abido, Optimal design of power-system stabilizers using particle swarm optimization, IEEE Trans. Energy Convers. 17 (3) (2002) 406–413.

[31] P.M. Anderson, A.A. Fouad, Power System Control and Stability, John Wiley & Sons, 2008.

[32] E.S. Ali, Optimization of power system stabilizers using BAT search algorithm, Int. J. Electr. Power Energy Syst. 61 (2014) 683–690.

[33] S.K.M. Kodsi, C.A. Canizares, Modeling and Simulation of IEEE 14 Bus System with Facts Controllers, University of Waterloo, Canada, Tech. Rep., 2003.

[34] L.H. Hassan, M. Moghavvemi, H.A. Almurib, K.M. Muttaqi, V.G. Ganapathy, Optimization of power system stabilizers using participation factor and genetic algorithm, , Int. J. Electr. Power Energy Syst. 55 (2014) 668–679.

[35] S.K. Wang, J.P. Chiou, C.W. Liu, Parameters tuning of power system stabilizers using improved ant direction hybrid differential evolution, Int. J. Electr. Power Energy Syst. 31 (1) (2009) 34–42.

[36] K.R. Padiyar, Power System Dynamics, BS Publications, 2008.

[37] A. Khodabakhshian, R. Hemmati, Multi-machine power system stabilizer design by using cultural algorithms, Int. J. Electr. Power Energy Syst. 44 (1) (2013) 571–580.

[38] A. Askarzadeh, A novel metaheuristic method for solving constrained engineering optimization problems: crow search algorithm, Comput. Struct. 169 (2016) 1–12.

[39] S. Mirjalili, A. Lewis, The whale optimization algorithm, Adv. Eng. Softw. 95 (2016) 51–67.

[40] R. Storn, K. Price, Differential evolution – a simple and efficient heuristic for global optimization over continuous spaces, J. Glob. Optimiz. 11 (4) (1997) 341–359.

[41] S. Mirjalili, S.M. Mirjalili, A. Lewis, Grey wolf optimizer, Adv. Eng. Softw. 69 (2014) 46–61.

Corresponding author
Aniruddha Bhattacharya can be contacted at: bhatta.aniruddha@gmail.com